Erschienen in: Lab on a Chip ; 16 (2016), 21. - S. 4152-4162
https://dx.doi.org/10.1039/c6lc00946h

Lab on a Chip

PAPER

View Article Online
View Journal | View Issue

Cite this: *Lab Chip*, 2016, **16**, 4152

Brain-on-a-chip model enables analysis of human neuronal differentiation and chemotaxis†

Onur Kilic,‡[a] David Pamies,‡[b] Emily Lavell,[c] Paula Schiapparelli,[c] Yun Feng,[cd] Thomas Hartung,[be] Anna Bal-Price,[f] Helena T. Hogberg,[b] Alfredo Quinones-Hinojosa,[c] Hugo Guerrero-Cazares*[c] and Andre Levchenko*[g]

Migration of neural progenitors in the complex tissue environment of the central nervous system is not well understood. Progress in this area has the potential to drive breakthroughs in neuroregenerative therapies, brain cancer treatments, and neurodevelopmental studies. To a large extent, advances have been limited due to a lack of controlled environments recapitulating characteristics of the central nervous system milieu. Reductionist cell culture models are frequently too simplistic, and physiologically more relevant approaches such as *ex vivo* brain slices or *in situ* experiments provide little control and make information extraction difficult. Here, we present a brain-on-chip model that bridges the gap between cell culture and *ex vivo*/*in vivo* conditions through recapitulation of self-organized neural differentiation. We use a new multi-layer silicone elastomer device, over the course of four weeks to differentiate pluripotent human (NTERA2) cells into neuronal clusters interconnected with thick axonal bundles and interspersed with astrocytes, resembling the brain parenchyma. Neurons within the device express the neurofilament heavy (NF200) mature axonal marker and the microtubule-associated protein (MAP2ab) mature dendritic marker, demonstrating that the devices are sufficiently biocompatible to allow neuronal maturation. This neuronal-glial environment is interfaced with a layer of human brain microvascular endothelial cells showing characteristics of the blood–brain barrier including the expression of zonula occludens (ZO1) tight junctions and increased trans-endothelial electrical resistance. We used this device to model migration of human neural progenitors in response to chemotactic cues within a brain-tissue setting. We show that in the presence of an environment mimicking brain conditions, neural progenitor cells show a significantly enhanced chemotactic response towards shallow gradients of CXCL12, a key chemokine expressed during embryonic brain development and in pathological tissue regions of the central nervous system. Our brain-on-chip model thus provides a convenient and scalable model of neural differentiation and maturation extensible to analysis of complex cell and tissue behaviors.

Received 25th July 2016,
Accepted 3rd October 2016

DOI: 10.1039/c6lc00946h

www.rsc.org/loc

1. Introduction

Cells migrate directionally in response to chemotactic gradients using a variety of sensing mechanisms and strategies, mostly in tissue culture models.[1–5] What happens in physiological settings in the presence of a complex tissue environment is far less clear.[6–9] Neural cell migration is a critically important mechanism underlying development of neural tissues that continues into adult life. During early embryonic brain development, cortical interneurons choreograph a complex pattern of migration to reach their targets, mediated by various chemokines such as CXCL12 (also known as SDF1).[10] In adult mammals, including humans, neuroblasts can migrate from the subventricular zone (SVZ) of the lateral ventricles to the olfactory bulb (OB) *via* the rostral migratory stream (RMS).[11–15] The regulation of cell migration through the RMS is an extremely complex process that involves a highly

[a] *Department of Biomedical Engineering, Johns Hopkins University, Baltimore, MD, USA*
[b] *Center for Alternatives to Animal Testing (CAAT), Johns Hopkins University, Baltimore, MD, USA*
[c] *Department of Neurosurgery and Oncology, Johns Hopkins University School of Medicine, Baltimore, MD, USA. E-mail: hugo@jhmi.edu*
[d] *Department of Pharmacology, School of Medical Science and Laboratory Medicine, Jiangsu University, Zhenjiang, People's Republic of China*
[e] *CAAT-Europe, University of Konstanz, Germany*
[f] *European Commission, Joint Research Centre, Institute for Health and Consumer Protection, Ispra, Italy*
[g] *Department of Biomedical Engineering and Yale Systems Biology Institute, Yale University, New Haven, CT, USA. E-mail: andre.levchenko@yale.edu*
† Electronic supplementary information (ESI) available. See DOI: 10.1039/c6lc00946h
‡ Equal contribution.

orchestrated interaction of intra- and extra-cellular signals.[16–20] In addition, under pathological conditions like ischemia or tumor growth, endogenous and exogenous neural progenitor cells (NPCs) are directed towards the damaged area. This is partially due to the effect of inflammatory chemokines such as CXCL12 (ref. 21, 22). Transplanted NPCs can home onto these pathological sites with great precision after migrating over long distances, *e.g.*, from the contralateral hemisphere.[21,23,24] All these findings point to a significant role of the cues provided by surrounding tissue in guiding these migratory cells over distances much longer than typically observed in *in vitro* studies. Thus, a better knowledge of the factors that regulate the migration of NPCs to damaged areas in the brain is necessary for successful cell and tissue regeneration or replacement therapies. However, for experimental information to be useful, it needs to be acquired in the environments that are sufficiently biomimetic. Current methods to study endogenous NPC migration include *in vivo* experiments that involve the injection of a tracing particle (nanoparticles, fluorescent markers, *etc.*) into the SVZ followed by the observations at an end point in the OB or accompanied by live imaging. These valuable methods are complex and expensive and are limited in the number of variables that can be modified at any given time. Experimental interventions commonly rely on the knockdown or overexpression of a single gene. On the other hand, common cell culture experiments, although far more controlled, often present a highly reductionist approach that might be unable to integrate the different environmental components that regulate cell migration. There is thus a pressing need for new controllable but biomimetic models of neural tissue development and function, including those incorporating the analysis of navigation of neural progenitors.

The past few years have seen a surge in interest in microfabricated devices that provide physiologically more relevant settings to address several shortcomings of standard *in vitro* models, especially 3D cultures[25] and further approximations of the organ situation.[26] Various microphysiological systems, sometimes referred to as organ-on-chips, have been demonstrated that allow culturing of multiple cell types in a controlled setting where mechanical and chemical conditions can be regulated and biological processes can be monitored with high fidelity.[27–29] These devices include brain-on-chip models that recapitulate aspects of the brain parenchyma[30–33] and also the blood–brain barrier (BBB).[34] However, due to the difficulty of culturing mature neurons, such as those within the central nervous system (CNS), these models commonly utilize prenatal or neonatal rodent cortical cells, which are then further matured within the device.[30–34] The results of such experiments are therefore necessarily interpreted in the context of the rodent cell origin, and present limited significance for the human physiology or pathology.

An attractive alternative to rodent brain cells can rely on differentiation of human neural stem cells within microphysiological devices. Neural stem cells provide an inexhaustible cellular resource, hence enabling scalable platforms. Furthermore differentiating neural stem cells into mature brain cells enables neurodevelopmental and neurotoxicology studies, and analysis of mature human neurons or glia. Despite these benefits, there are several challenges associated with microphysiological stem cell models. The fate of neural stem cells is highly sensitive to environmental cues. While microphysiological systems can provide a highly controlled environment, whether the level of control is sufficient to guide differentiation into healthy and mature neurons and glia is not clear, leading to limited utility of many of the currently used platforms and potential for inconsistency of the associated analyses.

In this study, we present a brain-on-a-chip platform that provides a controlled microenvironment that makes it possible to differentiate pluripotent human cells into mature neuronal and astroglial cells. To create a milieu mimicking the CNS, we differentiated pluripotent human NTera2 clone D1 (hNT2) cells inside highly structured silicone elastomer (polydimethylsiloxane) devices over a duration of several weeks into a mixed neuronal-glial cell population (NGCP) consisting of neuronal clusters interconnected with thick axonal bundles and interspersed with astrocytes. These results build on considerable promise of hNT2 cells that show NPC properties[35] and are able to differentiate into both neurons and astroglial cells after eight weeks of differentiation.[35–37] Besides reproducing the CNS morphology, hNT2 cells have been shown to also recapitulate neurotransmitter phenotypes, calcium channels, and electrophysiological activity,[38–40] hence provide a convincing and renewable alternative to primary human fetal neurons and astrocytes for mechanistic CNS studies.[41] The platform presented here shows that the differentiation of these cells can be enhanced and the resulting model tissues can be representative of mature CNS in terms of the tissue composition and organization. Using these brain-on-chip devices, we show that human fetal NPCs are able to respond to shallow CXCL12 gradients only in the presence of an environment consisting of neuronal networks and glial cells differentiated from hNT2 cells. Our brain-on chip platform, therefore, provides a model to study the effects of brain tissue on cell migration. Furthermore, in contrast to the standard *in vitro* approach of isolating cortical cells from animals, our platform recapitulates the differentiation process during early stages of nervous system development, and hence provides a novel tool to study neurodevelopment and developmental neurotoxicity.[42–45]

2. Materials and methods

2.1 Device design and fabrication

In vivo, CNS is composed of two critically important compartments: neural and vascular, with the neural tissue separated from the lumens of blood vessels with BBB. To recapitulate this brain tissue microenvironment, we fabricated a three-layer chip using a flexible and optically transparent material polydimethylsiloxane (PDMS). The top and bottom layers,

representing the scaffolds for modeling the lumens of the blood vessels and the neural tissue respectively, were separated by a middle porous PDMS membrane constituting an intermediate layer, as a scaffold for BBB (Fig. 1A). The top and bottom compartments could be perfused as channels of 5 mm width, 20 mm length, and 300 μm height. The top compartment had around 100 support pillars of 200 μm diameter each, distributed across the channel in a hexagonal array to prevent membrane collapse. The two compartments were separated by a 10 μm-thick PDMS membrane with 5 μm diameter holes. These PDMS chips were attached to glass coverslips, providing support and allowing high-resolution imaging. To allow for long-term cell culture, the devices were designed to be compatible with standard cell culture techniques. Funnel structures made of polypropylene tubes were cut to size and sterilized, and then pushed into the openings leading to the compartments (shown in Fig. 1B). For sterile and practical handling, the devices were then placed inside six-well plates (Fig. 1B). A cross-section of the final device that included the NGCP environment and the endothelial layer modeling BBB is shown in Fig. 1C.

The fabrication process is summarized in Fig. 1E and F. The PDMS devices were made using standard soft lithography techniques, whereby liquid prepolymer (10 : 1) was poured over a master and cross-linked at 80 °C for two hours. The master for the chips was fabricated using optical lithography using an epoxy-based negative photoresist (SU8) that yields thick and robust structures. In order to avoid toxicity issues due to non-crosslinked PDMS oligomers and residues of the platinum catalyst used to cure the PDMS, we cleaned the PDMS compartments through serial extractions and washes with several solvents as described previously.[46] The porous membranes were made by first coating PDMS prepolymer on a silanized master consisting of 15 μm high SU8 pillars, followed by pressing a fluoropolymer-coated polyester film (3M Scotchpak 1022 Release Liner) on the master using a c-clamp and curing the membranes overnight. After that, the polyester film with the attached porous PDMS membranes was peeled off from the master, and bonded to the top PDMS structure using an oxygen plasma (30 W, 700 mTorr, 30 s). After 2 hours of bonding, the polyester film was peeled off leaving the membrane attached to the top PDMS structure (Fig. 1E). To make the bottom compartment that has openings on both sides of the layer, a similar method was employed, whereby a fluoropolymer-coated polyester film was used to separate the structure from its master and bond to a glass coverslip using an oxygen plasma (Fig. 1F). Upon bonding of the three layers to each other, the chips were sterilized under intense UV light overnight.

2.2 Cell culture

2.2.1 Human teratocarcinoma NTERA-2 cl. D1 (hNT2) cells. hNT2 cell line was purchased from the American Type Culture Collection (Rockville, MD, USA). For maintenance and differentiation of the hNT2 cell line three different media (medium I–III in Table 1) were used according to the

Published on 03 October 2016.

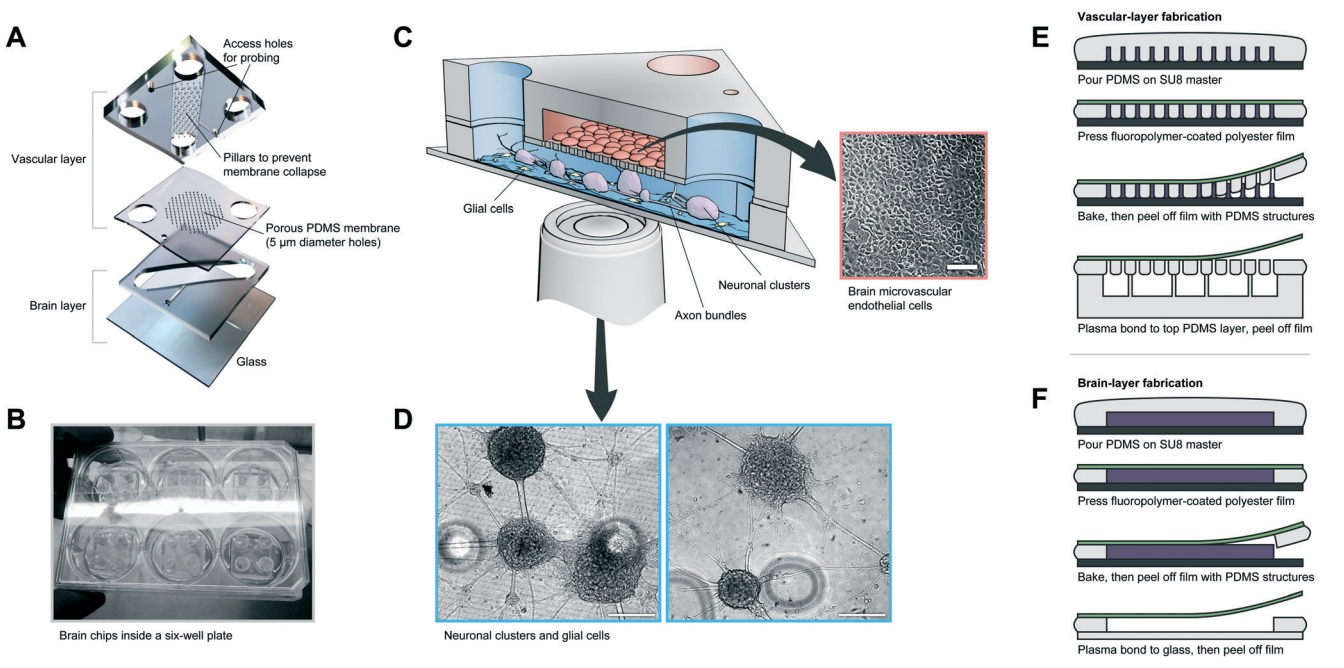

Fig. 1 Structure and fabrication of brain-on-chip platform. (A) Structure of device consisting of all-PDMS parts attached to glass. (B) Photograph of brain-chips in six-well plate format, compatible with standard pipetting techniques. (C) Cross-section of final brain-on-chip platform showing a NGCP layer consisting of human neuronal and glial cells, interacting through a perforated membrane with a monolayer of human brain microvascular endothelial cells (scale bar = 250 μm). (D) Brightfield image of the NGCP layer inside the devices (scale bars = 200 μm). (E and F) Fabrication process of the devices.

Table 1 Composition of hNT2 media

Medium I	Medium II	Medium III
Opti-MEM (Gibco)	DMEM-HG (Gibco)	DMEM-HG (Gibco)
5% heat-inactivated FBS (HyClone, Logan, UT, USA)	10% heat-inactivated FBS (HyClone)	10% heat-inactivated FBS (HyClone)
1% of penicillin–streptomycin–glutamine (100×) (Life technologies)	1% of penicillin–streptomycin–glutamine (100×) (Life technologies)	1% of penicillin–streptomycin–glutamine (100×) (Life technologies)
	10 μM retinoic acid (RA; Sigma, St. Louis, MO, USA)	Mitosis inhibitors (MI: 10 μM 5-fluoro-2′-deoxyuridine, 10 μM uridine, and 1 μM cytosine-β-D-arabino-furanoside)

protocol described by Pleasure *et al.*[37] A density of 3×10^6 neural progenitor hNT2 cells were seeded in uncoated 75 cm^2 flasks in medium I. After five weeks 2.3×10^6 hNT2 neuronal progenitor cells were seeded in uncoated 75 cm^2 flasks and kept for four weeks in medium II. During this time, retinoic acid (RA) was used to induce neuronal differentiation. After four weeks of RA treatment 500 000 cells were plated in the PDMS devices pre-coated with Matrigel (BD Biosciences, San Jose, CA, USA) and grown for four weeks in medium III containing mitosis inhibitors.

2.2.2 Human fetal neural progenitor cells (hNPCs). Primary human CNS tissue was obtained at gestational weeks 19–21. This was done under surgical written consent according to the National Institutes of Health Institutional Review Board Examp #5116 under Johns Hopkins University approved protocols based on its designation as pathological waste, as previously published.[47–50] Collected tissue was dissociated using gentle trituration in HBSS, centrifuged, washed and resuspended in neurobasal medium (NB) supplemented with B27 (Invitrogen). Cells were plated in NB +B27 and half media volume was changed twice per week. Cells were expanded, characterized, and kept growing in adherent culture in media containing DMEM with high glucose (Gibco 11985) Ham's F-12 (CellGro 10-080-CV), antibiotic, EGF and FGF (20 ng ml^{-1} each; Peprotech), and finally designated as cell line F54. To induce GFP expression, F54 cells were transfected with pCDNA-eGFP plasmid (Addgene) using lipofectamine, following manufacturer instructions.

2.2.3 Human brain microvascular endothelial cells (hBMECs). Following the differentiation of hNT2 cells inside the PDMS devices for four weeks (in medium III), immortalized hBMECs (a gift of the Piotr Walczak Laboratory[51]), were seeded on the membrane in the vascular layer of the devices (Fig. S3a†) and incubated using a medium composed of medium 199 (with glucose; Gibco) with added FBS (10%; Invitrogen) and antibiotic/antimycotic (1%) overnight to allow formation of a monolayer and to mimic the luminal surface of a blood vessel. Following the monolayer formation, the basal side was exposed to the brain-layer medium, and the hBMECs were cocultured with the brain layer for three days for maturation. To test nitric oxide (NO) synthesis, hBMEC cells were stimulated with VEGF (20 ng ml^{-1}; Peprotech). NO production was detected by infusing the cells with DAF-FM Diacetate dye (10 μM; ThermoFisher). To inhibit NO production, the cells were incubated (1 h, 37 °C) with the competitive NOS inhibitor L-NMMA (1 mM; SantaCruz) prior to loading the cells with DAF-FM Diacetate dye. L-NMMA was kept in the cell medium throughout incubation and experimental periods. hBMEC maturation was quantified using trans-endothelial electrical resistance (TEER) measurements every day over the course of six days using a multimeter and Ag–AgCl wire electrodes calibrated before each measurement (Fig. S3b and c†). The contribution of the device structure to the TEER measurements was accounted for by subtracting the resistance of the devices without cells.

2.3 Chemokine gradients

2.3.1 Gradient formation. The gradients were formed by diffusion[52] of human CXCL12 (Peprotech) and SLIT2-N (1093 amino acid glycoprotein corresponding to the N-terminal portion of the full length Slit2 precursor; Peprotech), peak concentration = 100 ng ml^{-1} for CXCL12, and 200 ng ml^{-1} for SLIT2-N. The gradients were stabilized for eight hours before the start of migration measurements. To quantify the concentration gradient profile of CXCL12, a tracer molecule (Texas Red-conjugated dextran, 25 μg ml^{-1} concentration, 10 kDa molecular weight) was introduced to one side of the bottom chamber. Fluorescence intensities of the tracer molecule were then recorded across the chamber over 12 hours using an Olympus IX81 microscope equipped with a Photometrics Cascade 512B II CCD camera, and processed using ImageJ.

2.3.2 Gradient simulation. To simulate the temporal and spatial profile of the gradients, the brain-chip devices were first modeled in 3D in COMSOL Multiphysics and subsequently solved with finite element analysis using the Transport of Diluted Species module. The diffusion coefficients of SLIT2-N and CXCL12 in water were taken as 0.5×10^{-10} m^2 s^{-1} and 1.4×10^{-10} m^2 s^{-1} respectively.

2.4 Chemotaxis analysis

2.4.1 Chemotactic cell introduction. For chemotaxis experiments two types of chips were used, denoted as control chips and brain chips. Brain chips were devices that included the brain-like NGCP layer, while control chips were empty chips devoid of any cells. To avoid possible effects of the perforated PDMS membrane on the gradient profile in the control chips, the vascular layer was not attached to the control

or brain chips during chemotaxis experiments, as depicted in Fig. 3. First, the control chips were coated with PLO+laminin. Then fetal hNPCs were introduced into both the control and brain chips (150 000 cells per chip) with attachment media (basic hNPC media without FGF/EGF/LIF, 10% serum, and 25 mM HEPES). After overnight attachment of hNPCs, the medium was changed for migration medium (same as the medium used for cell attachment but without serum). CXCL12 or SLIT2 dissolved in the migration medium was introduced on one side of the chip to form a gradient through diffusion,[52] and the gradient was stabilized for eight hours before the start of the migration measurements.

2.4.2 Time-lapse microscopy of live cells. Cell migration was tracked inside an enclosure with controlled temperature, humidity, and CO_2 using time-lapse microscopy (Movie S1†). To enable long-term observation, the control and brain chips were positioned inside a six-well plate that was mounted onto the stage of a motorized inverted microscope (Olympus IX81) equipped with a Photometrics Cascade 512B II CCD camera and temperature and gas controlling environmental chamber. Phase-contrast images were automatically recorded under a 10× objective (NA = 0.30) using the SlideBook 4.1 Software (Intelligent Imaging Innovations, Denver, CO) for 18 hours at 15 minute intervals (total of 72 frames for each imaging field).

2.4.3 Quantitative analysis of cell migration. A custom-coded MATLAB script was used to allow semi-automatic tracking of cell displacement frame by frame. The initial positions of the cells were set based on still GFP images taken at the beginning of the experiments, and the tracking was performed with phase-contrast images. Analysis was stopped in the event of cell death, cell division, or movement out of the field of view. Averages of migration parameters of cell populations were calculated from approximately 100 cells. Cell movements were tracked by centroid position or by the approximate center of the cell body. Individual cell trajectories were used to calculate the mean squared displacement (MSD) at each interval. Instantaneous speeds of individual cells were calculated from the MSD and the duration of the image acquisition time interval. Average speeds of individual cells were calculated from the total distance moved throughout the entire cell trajectory and the total time the cell was tracked. Persistence of individual cells was determined by calculating the ratio of the shortest distance between start and end points of the cell trajectory, divided by the total distance moved by the cell. Cell tracks, angular histograms, and chemotactic indices were calculated using Chemotaxis and Migration Tool 2.0 (Ibidi GmbH).

2.5 Immunofluorescence

Cells were first washed with PBS buffer and fixed for 15 min at room temperature (RT) with 4% paraformaldehyde. Following fixation, the cells were incubated for 1 hour at RT with PBS/0.1% Triton/10% goat serum on a shaker and further incubated overnight at 4 °C with primary antibodies (see Table 2) in PBS/0.1% Triton/2% goat serum. Then, cells were gently washed three times with PBS/0.1% Triton and incubated (1 hour at RT in the dark and with horizontal shaking) with fluorophore conjugated secondary antibodies (Alexa, Invitrogen) diluted 1 : 500 in PBS/0.1% Triton/2% goat serum. After secondary antibody incubation, cells were incubated for 10 min at RT with DAPI diluted at 1 : 5000 in water for staining the cell nuclei. Finally, cells were washed two times with 1× PBS. A Zeiss Observer microscope was used to take fluorescent images of the stained cells.

Table 2 List and specifications of antibodies used

Antibody	Host	Type	Source	Dilution
NF200	Rb	Polyclonal	Sigma N4142	1 : 200
MAP2ab	Mo	Monoclonal	Sigma M1406	1 : 500
NES	Rb	Polyclonal	Atlas HPA026111	1 : 500
GFAP	Rb	Polyclonal	Dako Z0334	1 : 500
TUJ1	Mo	Monoclonal	Covance MMS-435P	1 : 5000
CD31	Mo	Monoclonal	Cell signaling 3528	1 : 1000
ZO1	Mo	Monoclonal	Life technologies ZO1-1A12	1 : 100

3. Results and discussions

3.1 Brain-on-a-chip platform enables long-term culture of sensitive progenitor cells and differentiation of mixed neuronal-glial cell populations

The neurovascular unit, consisting of neurons, astrocytes, and vascular cells is essential to the function of the brain.[53] To model the brain microenvironment, we approximated this unit using a biocompatible brain-on-a-chip device that enables a co-culture of NGCP with a monolayer of brain microvascular endothelial cells (Fig. 1). The PDMS-based device consists of two compartments: one for neural cells, denoted as the "brain layer", and another one for endothelial cells, denoted as the "vascular layer" (Fig. 1A). The two compartments were separated by a porous PDMS membrane that allows cells on both sides to interact chemically and represents the scaffold for BBB. Before finalizing the device structure, we tested different structural layouts and fabrication methods so that long-term culturing (>4 weeks) of sensitive cell types was possible, as necessary for neuronal differentiation and maturation (see Discussion).

To generate a tissue environment that mimics the CNS, we established hNT2-derived NGCP cultures in the devices (Fig. 2B and S1a†). While arguably human fetal neurons and astrocytes would provide a more relevant setting for *in vitro* studies, the limited availability of these cell types and their non-renewable nature poses a significant problem for scalable microphysiological CNS models. Therefore, we instead used the well-characterized embryonal carcinoma cell line hNT2 capable of reproducing essential features of human neurons and astrocytes,[38–40] and hence providing a convincing and renewable alternative to primary human cells for mechanistic CNS studies.[41] To establish the NGCP culture, we started with undifferentiated hNT2 cells that were positive

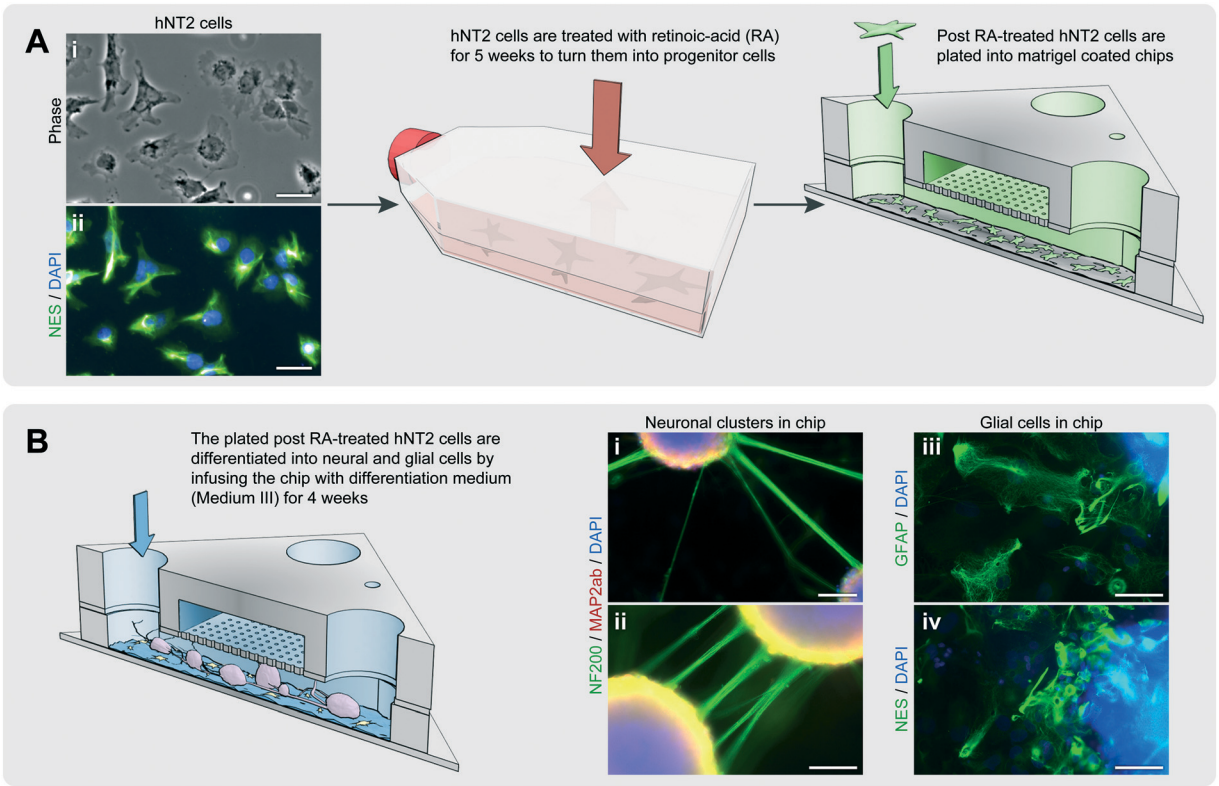

Fig. 2 hNT2 brain environment generation. (A) Diagram of RA-induction differentiation protocol. (A.i) shows phase contrast light image of undifferentiated hNT2 cells cultured on monolayer. (A.ii) shows neuronal precursor marker (Nestin, NES) immunostaining of undifferentiated hNT2 (scale bars = 100 μm). (B) Diagram shows postmitotic cell differentiation on the brain-on-a-chip platform. After 4 weeks with MI treatment cultures are shown to be positive to mature axonal marker (NF200, B.i and ii), mature dendritic marker (MAP2ab, B.i and ii), astrocytic marker (GFAP, B.iii), and neuronal precursor/astrocytes marker (NES, B.iv). DAPI was used for nuclear staining (scale bars = 100 μm).

for the neuroectodermal stem cell marker Nestin (NES), ensuring 100% NES-positive cells at this stage (Fig. 2A; before RA treatment). Following five weeks of retinoic acid (RA) treatment to induce neuronal differentiation, cells were plated into the lower chamber of the chip that was pre-coated with ECM (Matrigel). Maturation of RA-treated hNT2 cells inside the devices was facilitated by inhibiting proliferation using mitosis inhibitors (listed in Table 1) added to the cell media. Soon after seeding, cells attached to the ECM-coated glass surface and at 1 day *in vitro* (DIV) started to form small cell clusters (Fig. S2a†). Initial stages of the neuronal maturation process were observed after one week in the mitosis-inhibiting media, with cells forming larger clusters and extending neurite-like processes (Fig. S2b†). Four weeks of differentiation in the chips was sufficient to observe large cell clusters with thick neurite bundles (Fig. S2c†), which displayed high levels of the mature axonal marker neurofilament heavy (NF200) in the extended neurites, and mature dendritic marker microtubule-associated protein (MAP2ab) in the vicinity of the clusters (Fig. 2B), indicating a mature neuronal phenotype.[44,45] Neuronal maturation was further supported by electrophysiological activity measurements on neuronal clusters differentiated outside the chips under identical conditions (Fig. S1b†). Concurrent with neuronal differentiation and maturation, hNT2 cells that did not aggregate in the clusters assumed an astrocytic morphology and expressed glial fibrillary acidic protein (GFAP) (Fig. 2B). These results indicate that our devices provide a controlled microenvironment that allows hNT2 cells, representing an abundant cellular source, to differentiate simultaneously into neuronal and glial phenotypes, and thereby allowing a scalable platform to model key aspects of the CNS.

Subsequent to the maturation of the neuronal-glial layer, hBMECs were introduced to the top compartment to create a simple blood–brain barrier model. Monitoring of the hBMEC layer maturation and quantification of its barrier tightness was performed in control chips (n = 3) without the NGCP environment using trans-endothelial electrical resistance (TEER) measurements every day over the course of six days (Fig. S3†). As a control, human embryonic kidney 293 (HEK) cells were seeded on identical chips (n = 3) and their TEER data was compared to measurements from chips with hBMECs (Fig. S3c†). The measured resistance values indicate that hBMECs were able to form relatively tight barriers within less than a week of plating. This was further supported by immunofluorescence images of hBMECs grown under identical conditions on glass coverslips to allow high-resolution imaging, which showed expression of zonula occludens (ZO1) tight-junction markers and platelet endothelial cell adhesion molecule (CD31) (Fig. S3a†).

The functionality of the hBMEC layer was further validated by characterizing its functional response to vascular endothelial growth factor (VEGF) stimulation. In response to VEGF, functional endothelial layers are expected to produce nitric oxide (NO) through activation of NO synthase (NOS).[53] To image NO production, hBMEC cells were infused with DAF-FM Diacetate dye, a non-fluorescent cell permeable dye that becomes impermeable once inside the cell, and emits fluorescence after reacting with NO. Following VEGF stimulation, the hBMECs became fluorescent (Fig. S3a†), indicating NO production. To verify that NO was produced by NOS, hBMECs were incubated with the competitive NOS inhibitor L-NMMA, leading to markedly reduced NO production (Fig. S3a†). Taken together, these results indicate that the hBMEC layer in the chips displayed several important characteristics of the BBB. Further investigations are required to examine other properties of this model BBB in combination of model neural tissue.

3.2 Chemokine gradients in brain-on-a-chip platform induce specific cell migration

After establishing an *in vitro* CNS model using pluripotent human cells, we tested its applicability as a model to study tissue-guided chemotaxis of NPCs within the brain environment. *In vivo*, endogenous NPC migration is regulated by a complex interaction of internal and external factors.[16] While chemokines such as CXCL12 and SLIT2 are known to guide directional migration of NPCs, chemotaxis in the complex tissue environment is difficult to understand and investigate.[6–9] There are several factors that complicate the understanding of chemotaxis *in vivo*. Most chemokines have a multifunctional effect on both migrating cells and surrounding tissue. Also, chemokine distribution is difficult to assess due to formation of local gradients, and *in situ* gradients produced by migrating cells.[54] Furthermore, the interplay between contact inhibition of locomotion and short-range chemotaxis due to migrating cells interacting with each other or the surrounding tissue may lead to multicellular emergent behavior difficult to analyze.[55] Analysis of these complexities might be facilitated by more biomimetic platforms including the one described here. To investigate the effect of the NGCP environment on chemotaxis, fetal hNPCs expressing NES and to a lesser degree neuron-specific class III beta-tubulin (TUJ1) were introduced into the devices (Fig. 3A and B), and allowed to spread out and attach to the hNT2-based NGCP layer overnight. To distinguish them from the cells making up the NGCP environment in the chip, the hNPCs were transfected with GFP plasmids before introduction into the devices. Compared to control chips that lack the NGCP layer, the GFP-expressing hNPCs showed a substantially more polarized morphology in the brain chips (Fig. 3C). Following hNPC attachment, CXCL12 or SLIT2 was introduced on one side of the bottom chamber to allow formation and stabilization of a gradient through the brain layer (Fig. 3D). Finite-element simulation of the gradient profile in the brain chips for CXCL12 (Fig. 3E and F) and for SLIT2 (Fig. S4†) confirmed that relatively stable gradients are formed in the devices over extended time periods. The gradient profile for the CXCL12 concentration was quantified by the fluorescence intensity of a tracer molecule with similar molecular weight (Texas Red-conjugated dextran, 10 kDa) (Fig. 3G), which showed that the gradient developed within 4 hours, and remained relatively stable throughout the 12 hour measurement period.

After the formation of stable gradients, we performed a quantitative timelapse study of the migration of the hNPCs to understand how the presence of the NGCP environment affects chemotactic responses. The timelapse data showed largely stable hNPC migration speeds for both the brain chips and the control chips that lack the NGCP environment (Fig. 4A). However, hNPCs migrated significantly slower in the brain chips (almost 50% of control), independent of the type of gradient (Fig. 4B). Tracking of individual hNPCs (Fig. S5a†) and the angular histograms of the endpoints of these tracks (Fig. S5b†) showed that the hNPCs responded to the CXCL12 gradient only in the presence of the brain layer. The repulsive bias in the migration response in SLIT2 gradients was also observed only in the presence of NGCP, but the sample size was not sufficient to observe statistical significance in the overall chemotactic behavior. Comparisons of chemotactic index (difference between x-positions of start and end points, divided by the accumulated distance) showed that the directional chemotactic response of hNPCs was indeed only towards the shallow CXCL12 gradients exclusively in the presence of the NGCP layer (Fig. 4C). Furthermore, the measured persistence (shortest distance between start and end points divided by the accumulated distance) showed that cell migration exhibited a more consistent directionality in the presence of the NGCP layer (Fig. 4D). Collectively, these results indicate that hNPC cells show a stronger and more consistent response to chemotactic signals in the presence of the NGCP environment, suggesting that the long distance and highly persistent migration of NPCs observed *in vivo* in the brain tissue may be critically dependent on the cues arising from surrounding tissues. We believe that practical platforms as presented in this study provide the means for further investigation of the mechanical and chemical cues enhancing chemotactic responses.

3.3 Discussion

Despite the promise of organ-on-chip models, their impact on scientific research is still in its infancy. One of the barriers to widespread acceptance and implementation within the biomedical community is compatibility with existing infrastructure and methodologies.[27,28] Microphysiological systems should address the need to be usable without extensive training, and be compatible with standard culturing techniques such as micropipetting, plate readers, and automated handling systems. While there are many impressive organ-on-chip designs, the requirement of very specialized experience to operate the devices so far has hindered their large-

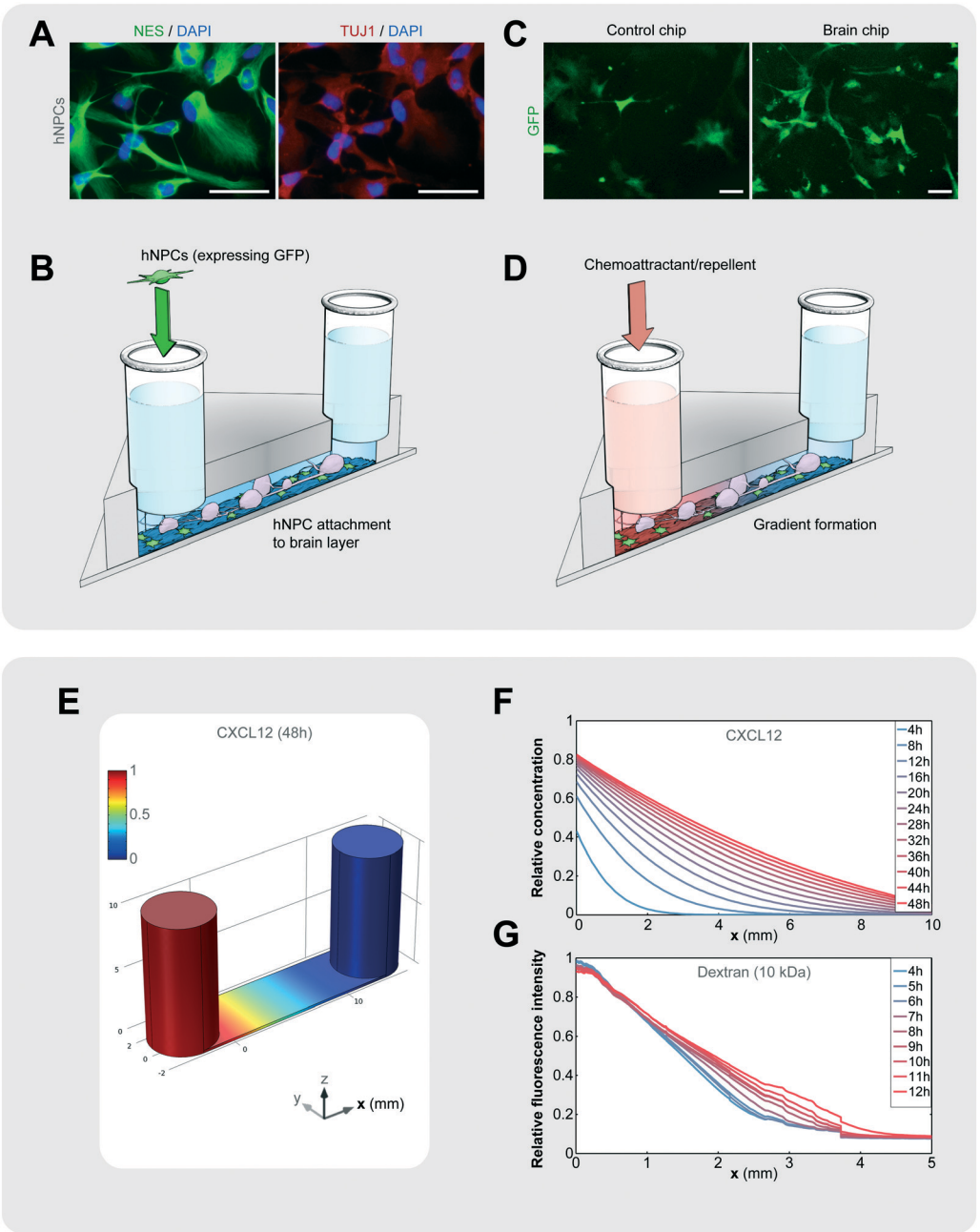

Fig. 3 Generation of chemotactic gradients in the brain chip. (A) The hNPCs express NES and to a lower degree neuron-specific class III beta-tubulin (TUJ1) (scale bars = 50 μm). (B) To distinguish from the cells making up the NGCP environment in the chip, hNPCs that are seeded into the brain layer express GFP. (C) Compared to a control chip that lacks the brain layer, the GFP-expressing hNPCs show a more polarized morphology in the brain chip (scale bars = 100 μm). (D) Following hNPC attachment, a chemoattractant or chemorepellent is introduced on one side to allow formation and stabilization of a gradient over time through the brain layer. Finite-element simulation of gradient evolution in the brain chips for CXCL12 (E and F) show relatively stable gradients over extended time periods. (G) The expected gradient profile was verified experimentally by the fluorescence intensity of a tracer molecule with a similar molecular weight (Texas Red-conjugated dextran, 10 kDa).

scale applicability and constrained them mostly as academic novelties. In this study, we took a user-centric route in designing the devices so that they could be handled by biologists untrained in microfluidic methods. In fact, the cells in this study were cultured in the devices for several weeks without difficulty by personnel that had never used microfluidic devices before.

Another barrier to broader acceptance of microphysiological CNS models is the requirement for scalability. Brain cells from animal resources are not inexhaustible, and also pose problems with regard to cross-species translation of results. In this study, we presented a PDMS-based brain-on-a-chip platform that makes it possible to differentiate pluripotent human cells into mature neuronal and astroglial cells.

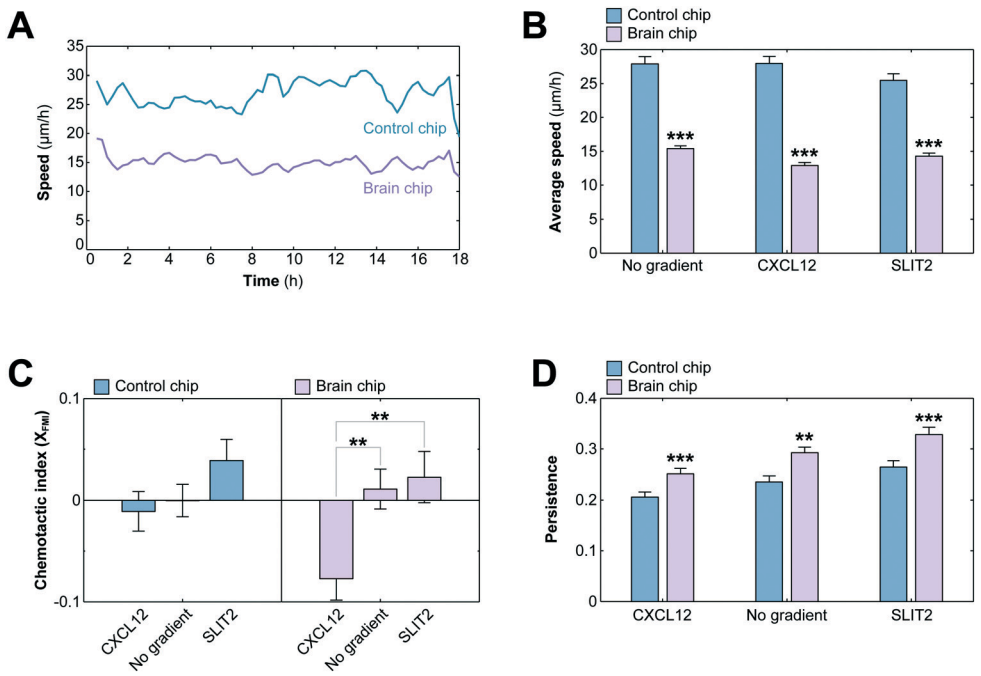

Fig. 4 Effect of brain layer on the chemotaxis of hNPCs. (A) Timelapse data shows relatively stable hNPC migration speeds for both the brain chips and the control chips lacking the brain layer. (B) hNPCs migrate significantly slower in the brain chips, independent of the type of gradient (no gradient, CXCL12, or SLIT2). (C) Comparisons of chemotactic index (aka forward migration index, *i.e.*, difference between *x*-positions of start and end points, divided by the accumulated distance) show that the hNPCs respond to the shallow CXCL12 gradients only in the presence of the NGCP layer. (D) Persistence (shortest distance between start and end points divided by the accumulated distance) is higher in the presence of the NGCP layer.

Published on 03 October 2016.

While PDMS-based microfluidic devices provide more precise control over the local microenvironment, there are several disadvantages compared to standard culturing techniques that makes maintaining and differentiating neural stem cells within microfluidic devices challenging. Besides user friendliness issues,[27,28] these challenges mainly stem from PDMS biocompatibility,[46,56,57] and the miniaturized culture environment impeding nutrient and gas exchange.[46,58] These issues not only affect viability, but also can lead to spontaneous differentiation of neural stem cells, preventing controlled mechanistic studies of neurodevelopment.[58] To address biocompatibility issues due to non-crosslinked oligomers and residues of the platinum catalyst used to cure the PDMS, we cleaned the device compartments through serial extractions and washes with several solvents as described previously.[46] To address nutrient and gas exchange issues, we designed compartments with >10 μl volumes and used a PDMS membrane instead of a standard thermoplastic membrane with lower gas permeability. These improvements over an initial device design led to a dramatic improvement of cell viability from 2–3 days to 4 weeks or more (results not shown).

To demonstrate that our brain-on-a-chip platform can be utilized in the analysis of physiologically relevant and clinically important problems, we introduced fetal hNPCs into the NGCP environment of our devices and observed how their migratory and chemotaxis behavior is affected. Neural cell chemotaxis is a cardinal feature of neural development and CNS tissue regeneration. It is also highly relevant for developmental neurotoxicity studies[59] and addressing problems in oncology, such as the role of brain tumor stem cell migration. Using an on-glass design allowed us to observe subcellular features with high resolution and dynamically track migrating hNPCs with high accuracy within stable chemokine gradients inside a shear-free environment. Our quantitative study revealed important insights into tissue-guided chemotaxis within the CNS. Specifically, we observed that hNPCs respond to shallow gradients of CXCL12 only in the presence of a microenvironment mimicking the brain parenchyma milieu. Furthermore, we observed that hNPCs were more polarized in the presence of the NGCP environment leading to more directed movement, a difference observed between 2D settings and 3D ECM settings.[60]

In summary, we designed a simple and user-friendly multi-layer silicone elastomer device, and optimized it for differentiation of pluripotent human cells into mixed population of mature neuronal and glial cells mimicking the CNS microenvironment. We also demonstrated that this brain tissue model could be extended to incorporate the blood–brain barrier, making it an attractive platform for a variety of neurotoxicity and drug delivery studies. This experimental platform allowed us to analyze cellular interactions between migrating hNPCs and the surrounding mature model brain tissue environment; something previously unexplored in *in vitro* settings, and meagerly researched in *in vivo* environments due to technical limitations. Our brain-on-chip model, therefore, provides a convenient tool for mechanistic studies

of various cell–cell interactions in a model CNS, which may shed light on important problems in neurodevelopmental studies, neurotoxicology, neuroregeneration, and neurooncology.

Acknowledgements

Part of this work was supported by grant R01NS070024 and by the Semiconductor Research Corporation's SemiSynBio program. OK was a recipient of the American Heart Association Postdoctoral Fellowship (13POST17140090).

References

1 M. Iijima, Y. E. Huang and P. Devreotes, Temporal and spatial regulation of chemotaxis, *Dev. Cell*, 2002, **3**(4), 469–478.
2 P. Devreotes and C. Janetopoulos, Eukaryotic chemotaxis: distinctions between directional sensing and polarization, *J. Biol. Chem.*, 2003, **278**(23), 20445–20448.
3 P. J. Van Haastert, Chemotaxis: insights from the extending pseudopod, *J. Cell Sci.*, 2010, **123**(18), 3031–3037.
4 R. H. Insall, Understanding eukaryotic chemotaxis: a pseudopod-centred view, *Nat. Rev. Mol. Cell Biol.*, 2010, **11**(6), 453–458.
5 C. Shi, C.-H. Huang and P. N. Devreotes, *et al.*, Interaction of motility, directional sensing, and polarity modules recreates the behaviors of chemotaxing cells, *PLoS Comput. Biol.*, 2013, **9**(7), e1003122.
6 M. D. Cahalan and I. Parker, Choreography of cell motility and interaction dynamics imaged by two-photon microscopy in lymphoid organs, *Annu. Rev. Immunol.*, 2008, **26**, 585.
7 J. Textor, A. Peixoto and S. E. Henrickson, *et al.*, Defining the quantitative limits of intravital two-photon lymphocyte tracking, *Proc. Natl. Acad. Sci. U. S. A.*, 2011, **108**(30), 12401–12406.
8 C. D. Sadik and A. D. Luster, Lipid-cytokine-chemokine cascades orchestrate leukocyte recruitment in inflammation, *J. Leukocyte Biol.*, 2012, **91**(2), 207–215.
9 P. Niethammer, C. Grabher and A. T. Look, *et al.*, A tissue-scale gradient of hydrogen peroxide mediates rapid wound detection in zebrafish, *Nature*, 2009, **459**(7249), 996–999.
10 Y. Wang, G. Li and A. Stanco, *et al.*, CXCR4 and CXCR7 have distinct functions in regulating interneuron migration, *Neuron*, 2011, **69**(1), 61–76.
11 F. Doetsch, J. M. García-Verdugo and A. Alvarez-Buylla, Cellular composition and three-dimensional organization of the subventricular germinal zone in the adult mammalian brain, *J. Neurosci.*, 1997, **17**(13), 5046–5061.
12 C. Lois, J.-M. Garcia-Verdugo and A. Alvarez-Buylla, Chain migration of neuronal precursors, *Science*, 1996, **271**(5251), 978–981.
13 C. Wang, F. Liu and Y.-Y. Liu, *et al.*, Identification and characterization of neuroblasts in the subventricular zone and rostral migratory stream of the adult human brain, *Cell Res.*, 2011, **21**(11), 1534–1550.
14 H. Guerrero-Cázares, O. Gonzalez-Perez and M. Soriano-Navarro, *et al.*, Cytoarchitecture of the lateral ganglionic eminence and rostral extension of the lateral ventricle in the human fetal brain, *J. Comp. Neurol.*, 2011, **519**(6), 1165–1180.
15 N. Sanai, T. Nguyen and R. A. Ihrie, *et al.*, Corridors of migrating neurons in the human brain and their decline during infancy, *Nature*, 2011, **478**(7369), 382–386.
16 V. Capilla-Gonzalez, E. Lavell and A. Quiñones-Hinojosa, *et al.*, Regulation of subventricular zone-derived cells migration in the adult brain, *Stem Cell Biology in Neoplasms of the Central Nervous System*, Springer, 2015, pp. 1–21.
17 N. Kaneko, O. Marín and M. Koike, *et al.*, New neurons clear the path of astrocytic processes for their rapid migration in the adult brain, *Neuron*, 2010, **67**(2), 213–223.
18 K. Sawamoto, H. Wichterle and O. Gonzalez-Perez, *et al.*, New neurons follow the flow of cerebrospinal fluid in the adult brain, *Science*, 2006, **311**(5761), 629–632.
19 K. J. Christie and A. M. Turnley, Regulation of endogenous neural stem/progenitor cells for neural repair—factors that promote neurogenesis and gliogenesis in the normal and damaged brain, *Front. Cell. Neurosci.*, 2012, **6**, 70.
20 J. C. Conover, F. Doetsch and J.-M. Garcia-Verdugo, *et al.*, Disruption of Eph/ephrin signaling affects migration and proliferation in the adult subventricular zone, *Nat. Neurosci.*, 2000, **3**(11), 1091–1097.
21 J. Imitola, K. Raddassi and K. I. Park, *et al.*, Directed migration of neural stem cells to sites of CNS injury by the stromal cell-derived factor 1α/CXC chemokine receptor 4 pathway, *Proc. Natl. Acad. Sci. U. S. A.*, 2004, **101**(52), 18117–18122.
22 D. Zagzag, M. Esencay and O. Mendez, *et al.*, Hypoxia-and vascular endothelial growth factor-induced stromal cell-derived factor-1α/CXCR4 expression in glioblastomas: one plausible explanation of Scherer's structures, *Am. J. Pathol.*, 2008, **173**(2), 545–560.
23 E. Y. Snyder, C. Yoon and J. D. Flax, *et al.*, Multipotent neural precursors can differentiate toward replacement of neurons undergoing targeted apoptotic degeneration in adult mouse neocortex, *Proc. Natl. Acad. Sci. U. S. A.*, 1997, **94**(21), 11663–11668.
24 K. S. Aboody, A. Brown and N. G. Rainov, *et al.*, Neural stem cells display extensive tropism for pathology in adult brain: evidence from intracranial gliomas, *Proc. Natl. Acad. Sci. U. S. A.*, 2000, **97**(23), 12846–12851.
25 N. Alepee, A. Bahinski and M. Daneshian, *et al.*, t4 Workshop Report: State-of-the-Art of 3D Cultures (Organs-on-a-Chip) in Safety Testing and Pathophysiology, *Altex*, 2014, **31**(4), 441.
26 T. Hartung, 3D—A new dimension of in vitro research, *Adv. Drug Delivery Rev.*, 2014, **69**, vi.
27 S. N. Bhatia and D. E. Ingber, Microfluidic organs-on-chips, *Nat. Biotechnol.*, 2014, **32**(8), 760–772.
28 E. W. Esch, A. Bahinski and D. Huh, Organs-on-chips at the frontiers of drug discovery, *Nat. Rev. Drug Discovery*, 2015, **14**(4), 248–260.

29 D. Pamies, T. Hartung and H. T. Hogberg, Biological and medical applications of a brain-on-a-chip, *Exp. Biol. Med.*, 2014, 1535370214537738.
30 A. Kunze, M. Giugliano and A. Valero, *et al.*, Micropatterning neural cell cultures in 3D with a multi-layered scaffold, *Biomaterials*, 2011, **32**(8), 2088–2098.
31 D. Majumdar, Y. Gao and D. Li, *et al.*, Co-culture of neurons and glia in a novel microfluidic platform, *J. Neurosci. Methods*, 2011, **196**(1), 38–44.
32 J. Park, H. Koito and J. Li, *et al.*, A multi-compartment CNS neuron-glia co-culture microfluidic platform, *J. Visualized Exp.*, 2009, **31**, e1399–e1399.
33 J. Park, B. K. Lee and G. S. Jeong, *et al.*, Three-dimensional brain-on-a-chip with an interstitial level of flow and its application as an in vitro model of Alzheimer's disease, *Lab Chip*, 2015, **15**(1), 141–150.
34 A. K. H. Achyuta, A. J. Conway and R. B. Crouse, *et al.*, A modular approach to create a neurovascular unit-on-a-chip, *Lab Chip*, 2013, **13**(4), 542–553.
35 P. W. Andrews, Retinoic acid induces neuronal differentiation of a cloned human embryonal carcinoma cell line in vitro, *Dev. Biol.*, 1984, **103**(2), 285–293.
36 S. Pleasure and V. Y. Lee, NTera 2 cells: a human cell line which displays characteristics expected of a human committed neuronal progenitor cell, *J. Neurosci. Res.*, 1993, **35**(6), 585–602.
37 S. J. Pleasure, C. Page and V. Lee, Pure, postmitotic, polarized human neurons derived from NTera 2 cells provide a system for expressing exogenous proteins in terminally differentiated neurons, *J. Neurosci.*, 1992, **12**(5), 1802–1815.
38 I. Guillemain, G. Alonso and G. Patey, *et al.*, Human NT2 neurons express a large variety of neurotransmission phenotypes in vitro, *J. Comp. Neurol.*, 2000, **422**(3), 380–395.
39 T. R. Neelands, A. P. King and R. L. Macdonald, Functional expression of L-, N-, P/Q-, and R-type calcium channels in the human NT2-N cell line, *J. Neurophysiol.*, 2000, **84**(6), 2933–2944.
40 R. S. Hartley, M. Margulis and P. S. Fishman, *et al.*, Functional synapses are formed between human NTera2 (NT2N, hNT) neurons grown on astrocytes, *J. Comp. Neurol.*, 1999, **407**(1), 1–10.
41 Y. Haile, W. Fu and B. Shi, *et al.*, Characterization of the NT2-derived neuronal and astrocytic cell lines as alternative in vitro models for primary human neurons and astrocytes, *J. Neurosci. Res.*, 2014, **92**(9), 1187–1198.
42 I. Laurenza, G. Pallocca and M. Mennecozzi, *et al.*, A human pluripotent carcinoma stem cell-based model for in vitro developmental neurotoxicity testing: effects of methylmercury, lead and aluminum evaluated by gene expression studies, *Int. J. Dev. Neurosci.*, 2013, **31**(7), 679–691.
43 G. Pallocca, M. Fabbri and M. G. Sacco, *et al.*, miRNA expression profiling in a human stem cell-based model as a tool for developmental neurotoxicity testing, *Cell Biol. Toxicol.*, 2013, **29**(4), 239–257.
44 D. Pamies, M. A. Sogorb and M. Fabbri, *et al.*, Genomic and phenotypic alterations of the neuronal-like cells derived from human embryonal carcinoma stem cells (NT2) caused by exposure to organophosphorus compounds paraoxon and mipafox, *Int. J. Mol. Sci.*, 2014, **15**(1), 905–926.
45 D. Pamies, A. Bal-Price and M. Fabbri, *et al.*, Silencing of PNPLA6, the neuropathy target esterase (NTE) codifying gene, alters neurodifferentiation of human embryonal carcinoma stem cells (NT2), *Neuroscience*, 2014, **281**, 54–67.
46 L. J. Millet, M. E. Stewart and J. V. Sweedler, *et al.*, Microfluidic devices for culturing primary mammalian neurons at low densities, *Lab Chip*, 2007, **7**(8), 987–994.
47 M. Zhu, Y. Feng and S. Dangelmajer, *et al.*, Human cerebrospinal fluid regulates proliferation and migration of stem cells through insulin-like growth factor-1, *Stem Cells Dev.*, 2014, **24**(2), 160–171.
48 A. L. Placone, P. M. McGuiggan and D. E. Bergles, *et al.*, Human astrocytes develop physiological morphology and remain quiescent in a novel 3D matrix, *Biomaterials*, 2015, **42**, 134–143.
49 A. F. Levy, M. Zayats and H. Guerrero-Cazares, *et al.*, Influence of basement membrane proteins and endothelial cell-derived factors on the morphology of human fetal-derived astrocytes in 2D, *PLoS One*, 2014, **9**(3), e92165.
50 R. Ravin, P. S. Blank and A. Steinkamp, *et al.*, Shear forces during blast, not abrupt changes in pressure alone, generate calcium activity in human brain cells, *PLoS One*, 2012, **7**(6), e39421.
51 M. F. Stins, F. Gilles and K. S. Kim, Selective expression of adhesion molecules on human brain microvascular endothelial cells, *J. Neuroimmunol.*, 1997, **76**(1), 81–90.
52 B. Lin and A. Levchenko, Spatial manipulation with microfluidics, *Front. Bioeng. Biotechnol.*, 2015, **3**, 39.
53 J. Madri, Modeling the neurovascular niche: implications for recovery from CNS injury, *J. Physiol. Pharmacol.*, 2009, **60**(Suppl 4), 95–104.
54 D. Cai and D. J. Montell, Diverse and dynamic sources and sinks in gradient formation and directed migration, *Curr. Opin. Cell Biol.*, 2014, **30**, 91–98.
55 B. Lin, T. Yin and Y. I. Wu, *et al.*, Interplay between chemotaxis and contact inhibition of locomotion determines exploratory cell migration, *Nat. Commun.*, 2015, **6**, 6619.
56 M. W. Toepke and D. J. Beebe, PDMS absorption of small molecules and consequences in microfluidic applications, *Lab Chip*, 2006, **6**(12), 1484–1486.
57 K. J. Regehr, M. Domenech and J. T. Koepsel, *et al.*, Biological implications of polydimethylsiloxane-based microfluidic cell culture, *Lab Chip*, 2009, **9**(15), 2132–2139.
58 B. Wang, S. Jedlicka and X. Cheng, Maintenance and Neuronal Cell Differentiation of Neural Stem Cells C17. 2 Correlated to Medium Availability Sets Design Criteria in Microfluidic Systems, *PLoS One*, 2014, **9**(10), e109815.
59 L. Smirnova, H. T. Hogberg and M. Leist, *et al.*, Food for Thought…: Developmental Neurotoxicity–Challenges in the 21st Century and In Vitro Opportunities, *Altex*, 2014, **31**(2), 129.
60 A. D. Doyle, F. W. Wang and K. Matsumoto, *et al.*, One-dimensional topography underlies three-dimensional fibrillar cell migration, *J. Cell Biol.*, 2009, **184**(4), 481–490.

